Journal of Advances and Scholarly Researches in Allied Education
Vol. 16, Issue No. 9, June-2019, ISSN 2230-7540

A Simple Braking Method for Six-phase Induction Motor Drives with Unidirectional Power Flow in the Base-Speed Region

M. J. Duran[1]* I. Gonzalez Prieto[2] F. Barrero[3] E. Levi[4] L. Zarri[5] M. Mengoni[6]

[1,2] Senior Member, IEEE, Department of Electrical Engineering, University of Malaga, Malaga, Spain

[3] Senior Member, IEEE, Department of Electronic Engineering, University of Seville, Seville, Spain

[4] Fellow Member, IEEE, School of Engineering, Technology and Maritime Operations in the Liverpool John Moores, Spain

[5] Senior Member, IEEE, Department of Electrical Engineering, University of Bologna, Bologna, Italy

[6] Member, IEEE, Department of Electrical Engineering, University of Bologna, Bologna, Italy

Abstract – Induction motor drives supplied from diode front-end rectifiers are commonly used in industrial applications due to their low cost and reliability. However, the two-quadrant operation of such a topology makes the regenerative braking impossible. Braking resistors can be used to dissipate the braking power and provide enhanced braking capability, but additional hardware is then necessary. Alternatively, the braking power can be dissipated within the inverter/motor by control software reconfiguration. In this scenario, the additional degrees of freedom of multiphase drives can be used to increase the system losses without disturbing the flux and torque production. Experimental results confirm the possibility to enhance the braking capability of six-phase drives with only few changes in the control scheme.

Index Terms—Multiphase Induction Motor Drives, Braking Methods, Field Oriented Control.

----------X----------

I. INTRODUCTION

The only efficient method to decelerate an induction motor is to operate in regenerative braking mode, sending the braking power back to the mains [1]. Nevertheless, regenerative braking requires bidirectional power flow, which is typically achieved using active front-end rectifiers and a back-to-back arrangement of voltage source converters (VSCs). Even though this topology is commonly used in high-power applications (traction and wind energy systems [2-5], to name a few), in many induction motor drives the use of diode front-end rectifiers is preferred due to the lower cost and improved reliability [6]. In such a case, the braking power cannot be delivered to the grid and needs to be absorbed somewhere. For dissipation purposes, it is possible to add an electronically controlled braking resistor across the dc-link, but it increases the cost, complexity and size of the drive [7]. Aiming to eliminate the power electronic components and electronic control circuits associated to this braking unit, different studies have investigated the braking capability of the drive without additional hardware [7-9, 12-13]. The main problem during rapid braking transients is that the kinetic energy of the power train flows to the dc-link. If the energy cannot be delivered back to the grid, then it increases the dc-link voltage. To avoid prohibitive overvoltage's in the dc bus, the braking power needs to be reduced and this slows down the deceleration process.

In this scenario, there is only one possible solution to enhance the braking power and speed up the deceleration process: to increase the system losses. Even though copper losses can be relatively small in high-power high-efficiency systems, they can significantly help the braking process in low- to medium-power induction motor drives [6-7]. Following this procedure, the drive serves itself as a virtual braking resistor, dissipating the braking power within the inverter/motor. The *dc-braking* [7] or the *high-slip braking* [8] are examples of strategies that aim to increase the braking torque by increasing the system losses. However, these methods are focused on stopping the motor rather than obtaining a high-performance braking operation. The rotor flux is very small in

both cases and this complicates the quick shift from braking to motoring mode of operation.

High performance braking methods are typically based on field oriented control (FOC) with some modifications to allow the generation of extra losses when requested. The most popular method is the *flux braking*, which increases the reference flux of the machine to induce extra losses and allow a controlled braking process [6-7, 9]. Interestingly enough, the strategy during braking is to make the motor as inefficient as possible within physical limits. While the flux is typically reduced in the base speed region to improve efficiency [1011], the flux should be increased during braking to worsen the efficiency and thus decelerate the motor faster.

However, high flux values over-magnetize the machine leading to magnetic noise in the base speed region and over voltages in the field weakening region [12]. The injection of current harmonics to induce losses has also been suggested in [13], but torque ripples become inevitable resulting in poor braking performance. A better performance is obtained by injecting a high-frequency square-wave superimposed to the *d*-current in such a manner that the impact on the torque ripple is minimized [12]. The control scheme is however complicated and it must be carefully designed to avoid coupling of the loss controller with the drive dynamics.

A common problem in all braking proposals for three-phase drives is that copper losses are increased by manipulating *d-q* currents and this causes disturbance in the flux and torque of the machine to some extent. A different situation is found in multiphase induction motor drives, where the phase redundancy naturally provides additional degrees of freedom [14-16]. Apart from the *d-q* currents, the vector space decomposition (VSD) [17] provides additional components in secondary planes, which are typically referred to as *x-y* components. These components allow the post-fault operation without extra hardware, and this fault tolerance is highly appreciated in safety-critical low-power applications such as in aircraft [18-20] or electric vehicle actuators [21]. While this capability is known from the early research studies in multiphase drives, other innovative uses for the new degrees of freedom have also appeared in recent times [6, 14, 22-24]. Since the braking mode of operation requires three degrees of freedom to independently regulate flux, torque and losses, an innovative use of the *x-y* currents is suggested in [25] to intentionally generate the losses. This induced inefficiency in turn helps the braking process in low-power drives with diode front-end rectifiers and means that the dynamic braking chopper, normally used in inverter fed drives, could be dispensed with. In higher power machines the stator resistance is typically lower but the current is higher. At the end of the day what matters is not the value of the stator resistance itself but the ratio of the copper losses ($\propto R_s I^2$) to the rated power of the machine. As the power increases, this ratio decreases because machines with higher power ratings typically have higher efficiency. Consequently, the method is generally valid for any power rating, but in the low-to-medium power range (say kW-range) the braking enhancement is higher and more effective than in the high-power range (say MW-range; however, in very high power region the braking is usually regenerative, achieved with a back-to-back converter connection). It is worth highlighting in any case that this feature is common to all methods that use the loss manipulation to help the braking process (e.g. in the loss manipulation strategy incorporated in DTC-based ABB drives [6] or those suggested in [7, 9, 12], to mention a few).

II. BACKGROUND OF THE BRAKING PROCESS IN INDUCTION MOTOR DRIVES

The equation of motion of an induction motor connected to a certain load is (assuming motoring convention further on):

$$T_e - T_L = J\frac{d\omega_m}{dt} + B\omega_m \qquad (1)$$

where T_e is the electrical torque, T_L is the load torque, J is the inertia of the power train, ω_m is the rotational angular speed of the motor and B is the friction coefficient. If the machine is operating with rated load, then the load torque is rated and this helps the deceleration process. However, if the load torque is low or is speed dependent (a typical characteristic is quadratic

dependence), the deceleration process becomes quickly far too slow. It is therefore customary to speed it up in a controlled manner by using negative values of the electrical torque (T_e<0). Fig. 1 represents this mode of operation with both electrical and load torque opposing the rotational direction to speed up the deceleration process. This implies in turn that the direction of the active power is reversed (Fig. 1) and the braking process takes place with P_{shaft}<0. This active power, simply referred to as the braking power from now on, flows through the motor and inverter and finally reaches the dc-link (P_{DC}). In the cases when

i. the drive is equipped with a diode front-end rectifier (Fig. 1) or

ii. the drive has an active front-end rectifier but there is voltage dip in the grid due to a fault the power cannot be delivered back to the grid and the dc-link voltage (V_{DC}) increases in an uncontrolled manner.

Since over voltages in the dc-link can quickly become prohibitive, it is necessary to brake the motor with P_{shaft}<0 (as in Fig. 1) but maintain P_{DC}> 0 (opposite direction as inFig. 1). This can only be

achieved by increasing the inverter and motor losses. A traditional method, commonly referred to as dc-braking, is to operate at zero stator frequency. Since the stator flux does not rotate, the air-gap power is zero ($P\ \delta$= 0), guaranteeing that the dc-link voltage is not increased (P_{DC} >0). Unfortunately, only rotor losses contribute to the braking process because the inverter and stator losses are not provided from the motor but from the grid side (P_s>0), resulting in a low braking power. Additionally, the deceleration is done in an uncontrolled manner, so it can be regarded as a stopping procedure rather than a high-performance braking method. A higher braking power is obtained if the stator power is zero (P_s= 0) since the stator copper losses are now provided from the machine and thus help the deceleration process [7-8]. A solution for zero stator power has been suggested in [8] operating at high-slip, but the solution is not integrated in a high-performance control scheme. Furthermore, the low flux found in this solution leads to poor dynamic performance and low iron losses. The other solution for P_s= 0 corresponding to low-slip operation is explored in [7], where a flux-braking approach is followed. As in [12], the braking method is integrated in a FOC-type strategy and losses are increased by injecting higher values of the d-current. Flux-braking methods however tend to over magnetize the machine and lack voltage capability in the high-speed region (especially in the field weakening region). Aiming to overcome such limitations, another high-performance braking method is to maintain the rated flux using constant average d-current but increase the copper losses using a high-frequency square-wave d-current injection [12]. Either the flux and/or torque are however disturbed in the aforementioned methods. To summarize, some desirable features of a braking strategy would be:

- The dc-link voltage should be kept below its limit.

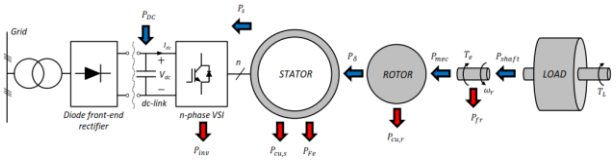

Fig. 1. Scheme of the power flow during the braking process in an induction motor drive with diode front-end rectifier. Blue arrows for power flow (negative values in motoring convention) and red arrows for losses. From left to right: P_{DC}= active power flowing to the dc-link, P_{inv}= losses in the inverter, P_s= electrical power supplied to the stator, $P_{cu,}$= stator copper losses, P_{Fe}= iron losses (neglecting rotor), $P\delta$= air-gap power, $P_{cu,r}$== rotor copper losses, P_{mec}= mechanical power, P_{fr}= windage and friction losses, P_{shaft} mechanical power at the motor shaft.

- System losses should be maximized, within voltage and current limits, to increase the braking power.
- All losses should be supplied by the machine, not by the inverter.
- The braking method must be integrated in a high-performance control and provide good dynamics when shifting from braking to motoring modes.
- Flux and torque should not be distorted by the loss manipulation strategy.
- Control scheme changes should be minimized.

III. A BRAKING STRATEGY FOR ASYMMETRICAL SIX-PHASE INDUCTION MOTOR DRIVES

A. Losses in Asymmetrical Six-phase Induction Motors:

Using the generalized Clarke's transformation [T] in its power-invariant form [5]:

$$[T]=\frac{1}{\sqrt{3}}\begin{bmatrix}1 & -\frac{1}{2} & -\frac{1}{2} & \frac{\sqrt{3}}{2} & -\frac{\sqrt{3}}{2} & 0\\ 0 & \frac{\sqrt{3}}{2} & -\frac{\sqrt{3}}{2} & \frac{1}{2} & \frac{1}{2} & -1\\ 1 & -\frac{1}{2} & -\frac{1}{2} & -\frac{\sqrt{3}}{2} & \frac{\sqrt{3}}{2} & 0\\ 0 & -\frac{\sqrt{3}}{2} & \frac{\sqrt{3}}{2} & \frac{1}{2} & \frac{1}{2} & -1\end{bmatrix} \quad (2)$$

$$[i_{\alpha s}\ i_{\beta s}\ i_{xs}\ i_{ys}]^T=[T]\cdot[i_{a1}\ i_{b1}\ i_{c1}\ i_{a2}\ i_{b2}\ i_{c2}]^T$$

the VSD-based electrical equations of an asymmetrical six-phase induction motor with distributed windings can be obtained from the phase variable model in the stationary reference frame as:

$$\begin{aligned}
v_{\alpha s}&=\left(R_s+L_s\frac{d}{dt}\right)i_{\alpha s}+M\frac{d}{dt}i_{\alpha r}\\
v_{\beta s}&=\left(R_s+L_s\frac{d}{dt}\right)i_{\beta s}+M\frac{d}{dt}i_{\beta r}\\
v_{xs}&=\left(R_s+L_{ls}\frac{d}{dt}\right)i_{xs}\qquad v_{ys}=\left(R_s+L_{ls}\frac{d}{dt}\right)i_{ys}\\
0&=\left(R_r+L_r\frac{d}{dt}\right)i_{\alpha r}+\omega_r L_r i_{\beta r}+M\frac{d}{dt}i_{\alpha s}+\omega_r M i_{\beta s}\\
0&=\left(R_r+L_r\frac{d}{dt}\right)i_{\beta r}-\omega_r L_r i_{\alpha r}+M\frac{d}{dt}i_{\beta s}-\omega_r M i_{\alpha s}\\
T_e&=pM(i_{\beta r}i_{\alpha s}-i_{\alpha r}i_{\beta s})
\end{aligned} \quad (3)$$

Where

$$L_s=L_{ls}+3L_m,\ L_r=L_{lr}+3L_m,\ M=3L_m,\ L_m$$

is the mutual inductance between stator and rotor phases and ω_r is the rotor electrical speed (ω_r = $p\omega_m$, p being the pole pair number).

It can be observed from (3) that the torque production is limited to the *a-ß* subspace, whereas the currents of the *x-y* subspace only generate copper losses in the stator. Additionally, *a-ß* and *x-y* planes are orthogonal and can be controlled independently. It is assumed that the six-phase machine has two isolated neutral points, so zero sequence currents are omitted from the analysis because they cannot flow. For control purposes, the *a-ß* subspace is typically rotated using the Park rotational transformation:

$$[D] = \begin{bmatrix} cos\theta_s & sin\theta_s \\ -sin\theta_s & cos\theta_s \end{bmatrix} \quad (4)$$

that provides the *d* and *q* components, used for flux and torque regulation, respectively.

Core losses caused by eddy currents and hysteresis, neglected in (3), are dependent on the stator flux and frequency. Consequently high iron losses are obtained if the flux is maintained at rated value by setting $i_{ds}^{*} = i_{dsn}$. This also ensures good dynamic performance of the drive when transiting from braking to motoring mode of operation.

Copper losses depend on the stator currents in the form:

$$P_{cu} = P_{cu,s} + P_{cu,r} = R_s\left(i_{ds}^2 + i_{qs}^2 + i_{xs}^2 + i_{ys}^2\right) + R_r i_{qs}^2 \quad (5)$$

Since either the torque loop of the field oriented control or the limitations imposed on the braking power would set the *q* current reference (iq^*), both *d* and *q* currents are fixed by the regulation of flux and torque, respectively. Fortunately, in the asymmetrical six-phase machine one can still manipulate the copper losses by proper injection of the *x-y* currents.

B. Injection of x-y currents for loss manipulation:

The main idea to perform a safe braking is to divert the energy that would typically be delivered to the dc-link by manipulating the *x-y* losses. Let us consider the qualitative example of a machine that is driven at speed n_1 and it is decelerated down to n_2 in a ramp-wise manner (Fig. 2a). When the machine starts the deceleration at time t_0, the dc-link power is quickly reversed to absorb the kinetic energy (Fig. 2b), and this causes the rise of the dc-link capacitor voltage. Alternatively, the energy that would be delivered to the dc-link (shaded area in Fig. 2b) can be dissipated as *x-y* copper losses (shaded area in Fig. 2d). This keeps the dc-link power always positive, as shown in Fig. 2c. At time t_1 the deceleration process comes to an end and the injection of the *x-y* current is no longer necessary (Fig. 2d). The power profile of Fig. 2b is the subtraction of those in Fig. 2c and 2d, and for this reason the dynamics during the transient are not altered.

From the machine model (3) it can be noted that:

i. the injection of x-y currents does not disturb the flux and torque;

ii. the regulation of the x-y currents can be done independently from the flux/torque control (due to the orthogonally of *a-b* and x-y subspaces);

iii. the x-y currents can be injected in a quick manner due to a low electrical time constant;

iv. low x-y voltage is required for the current injection because the impedance in the x-y plane is low. Consequently, the loss control through the x-y currents becomes an ideal candidate to improve the braking process.

The amount of *x-y* currents that can be tolerated directly depends on the current and voltage constraints of the system. Current constraints are typically more restrictive at low speed whereas prohibitive voltages are found at high speed, especially in the field-weakening region. This work focuses on the operation in the base speed region and will only consider current constraints. The stator currents are limited by the ratings of both the motor and inverter. However, the induction motors can handle typically up to four times their nominal rms currents (I) for short periods of time. This overload capability is normally quantified by manufacturers when the induction motor operates in interment duties and during direct online (DOL) starting. Considering that the *x-y* current injection is performed only during sudden decelerations, the current limit in this transient state is practically constrained by the inverter rating [8]. Since inverters typically incorporate some overload capability for short-time acceleration at higher than rated torque, it is likely that the maximum current that can be tolerated during the braking transient is higher than rated ($I_{max} = \alpha I_n, \alpha > 1$) still keeping the motor on the safe side with no concerns about thermal effects. Considering that copper losses increase with the square of the current, it is important to take advantage of such overload transient capability (e.g. α = 1.5 results in 225% copper losses). Some current capability is reserved for the flux and torque production with *d-q* currents, but the *x-y* currents can be injected up to the limit set by the maximum per leg rms inverter current (I_{max}):

$$i_{sx}^2 + i_{sy}^2 \leq 6I_{max}^2 - i_{sd}^2 - i_{sq}^2 \quad (6)$$

An important remark is that the current limit in (6) is only valid for the case when phase currents are balanced. Although this is the standard case in motoring operation due to the zero value of x-y currents, it may not hold true if x-y currents are not injected in a proper manner. This would provide a

suboptimal solution and consequently needs some further analysis.

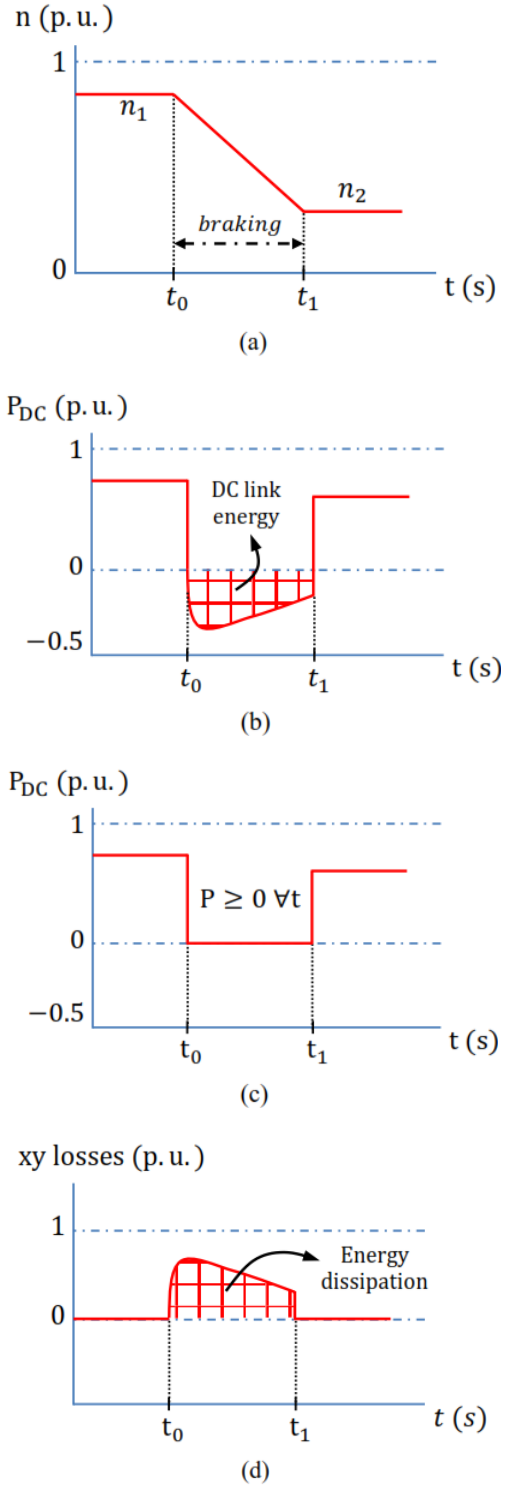

Fig. 2. Qualitative explanation of the energy dissipation during the braking process: (a) Speed, (b) Dc-link power with no x-y energy dissipation, (c) Dc-link power with x-y energy dissipation, (d) x-y injection during the braking transient.

Considering the inverse of the Clarke's transformation matrix, the phase currents can be written as:

$$
\begin{aligned}
i_{a1} &= (i_{\alpha s} + i_{xs})/\sqrt{3} \\
i_{b1} &= \left(-\frac{1}{2}i_{\alpha s} + \frac{\sqrt{3}}{2}i_{\beta s} - \frac{1}{2}i_{xs} - \frac{\sqrt{3}}{2}i_{ys}\right)/\sqrt{3} \\
i_{c1} &= \left(-\frac{1}{2}i_{\alpha s} - \frac{\sqrt{3}}{2}i_{\beta s} - \frac{1}{2}i_{xs} + \frac{\sqrt{3}}{2}i_{ys}\right)/\sqrt{3} \\
i_{a2} &= \left(\frac{\sqrt{3}}{2}i_{\alpha s} + \frac{1}{2}i_{\beta s} - \frac{\sqrt{3}}{2}i_{xs} + \frac{1}{2}i_{ys}\right)/\sqrt{3} \\
i_{b2} &= \left(-\frac{\sqrt{3}}{2}i_{\alpha s} + \frac{1}{2}i_{\beta s} + \frac{\sqrt{3}}{2}i_{xs} + \frac{1}{2}i_{ys}\right)/\sqrt{3} \\
i_{c2} &= -(i_{\beta s} + i_{ys})/\sqrt{3}
\end{aligned}
\qquad (7)
$$

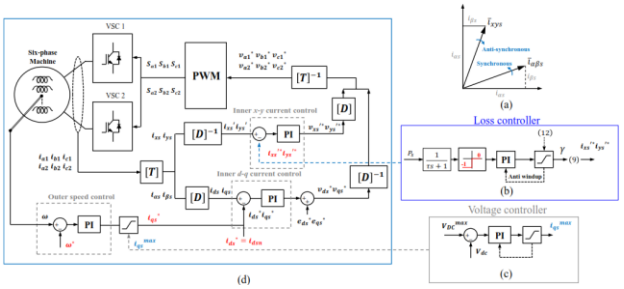

Fig. 3. Control strategy. (a) Synchronous and anti-synchronous rotation of *a-ß* and *x-y* current space phasors according to condition (7) with γ = 1, (b) Loss controller for *x-y* current reference generation, (c) Dc-link voltage controller and (d) Field oriented control (FOC) of the six-phase induction motor.

A solution that satisfies the requirement of equal magnitude in phase currents is:

$$
\begin{aligned}
i_{xs} &= \gamma i_{\beta s} \\
i_{ys} &= \gamma i_{\alpha s}
\end{aligned}
\qquad (8)
$$

where γ is a parameter that regulates the amount of current injection and provides the additional copper losses that are necessary for the braking process:

$$P_{cu} = P_{cu,s} + P_{cu,r} = (1+\gamma^2)R_s\left(i_{sd}^2 + i_{sq}^2\right) + R_r i_{qs}^2 \qquad (9)$$

Equation (7) also implies that both the space phasors in the *a-ß* subspace $(\bar{\imath}_{\alpha\beta s} = i_{\alpha s} + j i_{\beta s})$ and in the *x-y* subspace $(\bar{\imath}_{xys} = i_{xs} + j i_{ys} = \gamma(i_{\beta s} + j i_{\alpha s}))$ rotate at fundamental frequency, but in opposite directions. While $\bar{\imath}_{\alpha\beta s}$ αs rotates in synchronous direction, $\bar{\imath}_{xys}$ rotates in anti-synchronous direction, as schematically indicated in Fig. 3a.

It is worth noting that the injection of the x-y currents can be done with low values of the x-y voltages because the impedance of the x-y plane is low in distributed winding machines. The value of $L_{ls} \ll L_m$ and for this reason $|Z_{xy}| \ll |Z_{dq}|$. For the sake of example, with the machine parameters in [16] the value of $|Z_{xy}|$ at 50 Hz is only 6% of the no-load impedance.

A. Design of the loss controller:

It is firstly necessary to decide the frame of *x-y* currents where the control would be optimally performed. Since it has been already shown that the condition of balanced operation (6) implies an anti-synchronous rotation of $\bar{\imath}_{xys}$, it follows that the choice of a synchronous reference frame using Park transformation [D] would generate sinusoidal *x-y* currents at twice the fundamental frequency. This would require the use of controllers with a wide bandwidth or resonant controllers, which may complicate the control structure and tuning.

Alternatively, the choice of an anti-synchronous reference frame using $[D]^{-1}$ provides constant x-y currents and allows the use of simple proportional-integer (PI) x-y controllers. By selecting a synchronous reference frame for d-q currents and an anti-synchronous reference frame for the x-y currents, the condition (8) is transformed into:

$$\begin{aligned} i_{xs}' &= \gamma i_{qs} \\ i_{ys}' &= \gamma i_{ds} \end{aligned} \qquad (10)$$

where i_{xs}' and i_{ys}' denote the x-y current components after the anti-synchronous rotation.

Considering the relationship between components used in the VSD (d-q-x-y) and double d-q (d_1-q_1-d_2-q_2) approaches [5]

$$\begin{aligned} i_{ds} &= \sqrt{1/2}\,(i_{d1s} + i_{d2s}) \quad i_{ds} = \sqrt{1/2}\,(i_{d1s} + i_{d2s}) \\ i_{xs}' &= \sqrt{1/2}\,(i_{d1s} - i_{d2s}) \quad i_{ys}' = \sqrt{1/2}\,(i_{q2s} - i_{q1s}), \end{aligned} \qquad (11)$$

the expression in (10) can be rewritten in terms of the *d-q* components of windings 1 and 2 as:

$$\begin{aligned} i_{d1s} &= \frac{i_{ds} + \gamma i_{qs}}{2} \quad i_{d2s} = \frac{i_{ds} - \gamma i_{qs}}{2} \\ i_{q1s} &= \frac{i_{qs} - \gamma i_{ds}}{2} \quad i_{q2s} = \frac{i_{qs} + \gamma i_{ds}}{2} \end{aligned} \qquad (12)$$

The condition (8) is a mathematical solution to obtain balanced current operation, but (12) provides a further insight into this solution with a clear physical meaning: in motoring operation (γ = 0) the contribution of windings 1 and 2 to the flux and torque production is equal but for increasing values of γ winding 1 contributes more to the flux creation whereas winding 2 becomes torque-related. Consequently, phase currents remain balanced during braking but the nature of these currents is modified to worsen the efficiency, and this is reflected in the rise of *x-y* currents.

The amplitude and phase shifting of the *d-q* phasors of windings 1 and 2 are:

$$\begin{aligned} |i_{dq1s}| &= |i_{dq2s}| = \frac{1}{2}\left[(1+\gamma^2)i_{ds}^2 + (1+\gamma^2)i_{qs}^2\right]^{\frac{1}{2}} \\ \varphi_{12} &= \tan^{-1}\left(\frac{\gamma i_{ds} + i_{qs}}{i_{ds} - \gamma i_{qs}}\right) - \tan^{-1}\left(\frac{i_{qs} - \gamma i_{ds}}{\gamma i_{qs} + \gamma i_{ds}}\right) \end{aligned} \qquad (13)$$

confirming that conditions (8) and (10) provide a balanced operation with variable phase shifting between the three-phase currents of windings 1 and 2.

The limit (6) can now be expressed in terms of the current injection parameter γ:

$$\gamma \leq \sqrt{\frac{6I_{max}^2}{i_{ds}^2 + i_{qs}^2} - 1} \qquad (14)$$

The second issue to consider is the instant when *x-y* currentsshould be injected. The actual instant when the power is being delivered to the dc-link, thus initiating the rise of V_{DC}, is when the dc-link power becomes negative (P< 0). Unfortunately, the determination of this condition requires the measurement of the dc-link current I_{DC}, which is typically not incorporated in induction motor drives. Consequently, the proposed condition for the activation of the loss controller is the reversal of the stator power, that is, when P_s< 0. The stator power can be expressed in terms of VSD variables as:

$$P_s = v_{\alpha s} i_{\alpha s} + v_{\beta s} i_{\beta s} + v_{xs} i_{xs} + v_{ys} i_{ys} \qquad (15)$$

Next, it is also necessary to decide the inputs and outputs of the controller. The variable γ from (8) and (10) is used as an output since it allows the rise of copper losses (9) and provides balanced operation (13). P_s is selected as the input because the aim of the loss controller is to maintain the stator power above a certain threshold (typically $P_{threshold}$ = 0) to avoid dc-link power reversal. The controller includes a low-pass filter for P_s to provide smoother operation and an anti-windup PI controller with saturation set by (14). The designed loss controller is finally shown in Fig. 3b, which needs to be integrated in the FOC scheme.

B. Overall control strategy:

The complete control scheme is shown in Fig. 3. It comprises three different parts:

- The field oriented control used for motoring mode of operation (Fig. 3d). This part of the control scheme uses a conventional scheme with an outer speed loop and inner control loops to regulate the VSD currents. The *q*-current reference is provided by the speed loop and the *d*-current reference is set to a constant value to operate at rated flux in the base speed region. The regulation of *d-q* currents is performed in

the synchronous reference frame whereas the regulation of the *x-y* currents is performed in ant synchronous reference frame. PI controllers are used for both *d-q* and *x-y* components. The reference for the *x-y* currents is set by the loss controller of Fig. 3b. Inner current controllers provide the voltage references v_{ds}^{*}, v_{qs}^{*} and $v_{xs}^{\prime *}, v_{ys}^{\prime *}$ that are converted back to the stationary frame using Park $[D]$ and inverse Park $[D]^{-1}$ transformations, respectively. Inverse Clarke transformation $[T]^{-1}$ is then used to obtain the phase voltage references that are finally fed to the carrier-based PWM stage.

- The loss controller (Fig 3b), which is integrated in the FOC scheme to provide zero *x-y* current references in motoring operation *(P_s>$P_{threshold}$=0)* and non-zero values during braking *(P_s<$P_{threshold}$=0)*. Since the loss controller already inputs a zero value when *(P_s>$P_{threshold}$ = 0)*, there is no need to switch the controller off during motoring operation. This provides a simple and smooth activation/deactivation of the loss controller when required.

- The loss controller, shown in Fig 3b, which is integrated in the FOC scheme to provide zero *x-y* current references in motoring operation *(P_s>$P_{threshold}$=0)* and non-zero values during braking *(P_s<$P_{threshold}$=0)*. Since the loss controller already inputs a zero value when *(P_s>$P_{threshold}$ = 0),* there is no need to switch the controller off during motoring operation. This provides a simple and smooth activation/deactivation of the loss controller when required.

The voltage controller (Fig. 3c). Even though the loss controller of Fig. 3b will help to some extent the braking process, the loss generation capability is limited by (12). Once this saturation is reached, it is then necessary to include a dc-link voltage controller to limit the amount of regenerative power that is being reversed. This limitation is simply done by a PI controller that takes the dc-link voltage error as an input and sets a limit for the *q*-current reference as an output [12].

A. Test bench:

The different elements of the test rig that has been used for the experimental testing is shown in Fig. 4. The six-phase drive consists of an asymmetrical six-phase induction machine driven by conventional two-level three-phase VSCs from Semikron (SKS22F modules). Ac-time domain and stand-still with inverter supply tests [26-27] have been used to determine the parameters of the custom-built multiphase machine. Table I shows the induction motor drive parameters and rated values. The VSCs are connected to a single dc power supply and the control actions are performed by a digital signal processor (TMS320F28335 from Texas Instruments, TI). The control unit is programmed using a JTAG and the TI proprietary software Code Composer Studio.

Table I

Induction Motor Drive Parameters and Test-Bench Rated Values

Power (kW)	0.4
Dc-link voltage (V)	300
Switching frequency (kHz)	10
I_{peak} (A)	2.6
i_d (A)	1.1
i_q (A)	3
n_m (rpm)	1000
R_s (Ω)	4.2
R_r (Ω)	2
L_m (mH)	420
L_{ls} (mH)	4.2
L_{lr} (mH)	55
R_{load} (Ω)	25

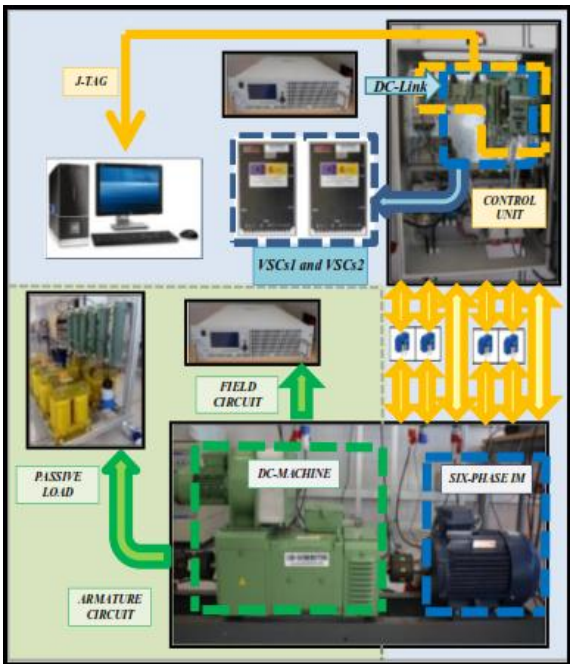

Fig. 4: Scheme of the test bench used for the experimental results.

Four hall-effect sensors (LEM LAH 25-NP) and a digital encoder (GHM510296R/2500) have been used to obtain the current and speed measurements, respectively. A dc machine is coupled to the shaft of the six-phase induction motor in order to perform load tests. The armature of the dc machine is connected to a variable passive *R* load that dissipates the power and the load torque is consequently speed-dependent.

B. Experimental results:

This section experimentally verifies that the injection of *x-y* currents during the braking transient can effectively maintain the electrical power supplied to the stator above a certain threshold. This prevents the power reversal that eventually provokes the rise of the dc-link voltage. As discussed in sections II and III, the problem commences when the power is reversed during the braking transient and consequently the threshold for the activation of the *x-y* current injection is set to zero (Fig. 2c and 3b). Nevertheless, for security reason in the laboratory this threshold is set to 70W, so the aim of the control strategy is to maintain the input power above $P_{threshold}$.

In order to prove the capability of the loss controller to limit the stator power above $P_{threshold}$, the same test is done without (Fig. 5) and with (Fig. 6) the activation of the *x-y* current injection of Fig. 3b. In the test the six-phase machine is driven in steady-state at 250 rpm and the speed reference is then decreased in a ramp-wise manner at t = 5s down to 150 rpm. Both tests are done by setting a *d*-current of 1.1A, with a switching frequency of 10 kHz and a dc-link voltage of 300V. Fig. 5a shows a satisfactory speed tracking of the machine both in steady-state and during the deceleration transient. The *d*-current is constantly regulated to 1.1A and it is fully decoupled from the *q*-current, which is decreased during the transient to fulfill the dynamic requirements (Fig. 5b). The *x-y* currents are regulated to zero (Fig. 5c) because the controller of Fig. 3b is not activated and consequently γ = 0 throughout the test (Fig. 5e). However, the slope of the deceleration ramp that is initiated at t = 5 is high enough to make the stator power (Ps) drop below the threshold of 70W as it can be observed in the zoom-in detail of Fig. 5d.

When the *x-y* current injection of Fig. 3b is activated it is still possible to satisfactorily regulate the speed and *d-q* currents (Fig. 6a and 6b). However, the activation of the *x-y* current injection during the braking transient (Fig. 6c) maintains the stator power above the threshold of 70W even during the deceleration process (Fig. 6d). The value of γ is zero while the stator power is above $P_{threshold}$, but at approximately t = 6 the stator power falls below this limit. Then, a non-zero current injection parameter γ is provided by the controller shown in Fig. 3b and this allows the *x-y* current injection during the last part of the braking process (from t =6.05s to t = 6.3s as it can be observed in the zoom-in detail of Fig. 6e). As expected, no further current injection is obtained after the deceleration process. While the braking power and the dynamics are the same in Figs. 5 and 6, the *x-y* current injection is the key to dissipate the extra power. The additional copper losses permit to keep the stator power above the threshold and avoid the eventual rise of the dc-link capacitor voltage.

To summarize, the transient *x-y* current injection has the following properties:

- It is fully decoupled from the *d-q* current tracking (Fig. 6b) and consequently it does not disturb the flux/torque production.
- It does not affect at all the speed dynamics during the braking transient (Fig. 6a).
- It can be performed in a quick manner due to the low electrical time constant (Fig. 6c).
- It maintains the stator power that is supplied to the motor above a certain threshold (Fig. 6d).
- It requires low voltage requirements due to the low impedance of the *x-y* plane (Fig. 6f).
- It keeps changes in the control strategy to a minimum, just adding the controller of Fig. 3b.

These features are in accordance with the desired characteristics listed in section II and consequently prove that inducing machine losses with the suggested method can be an effective way to help the braking transient and to avoid eventual dc-link over-voltages.

V. CONCLUSIONS

Electrical drives with unidirectional power flow and without braking resistors can only improve their braking capability by transiently inducing extra losses in the system. This work presents an innovative use of the additional degrees of freedom that exist in six-phase drives and allow generation of extra copper losses during the braking process without disturbing the flux and torque production. A loss controller is included into the field oriented control providing a simple and effective manner to enhance the braking capability. Compared to previous methods used in three-phase drives, three main distinctive features can be highlighted in relation to the proposed technique:

- It is possible to independently regulate the drive losses without disturbing the flux and torque production. Consequently, the dynamics of the drive are not affected and there is no risk of over magnetizing the machine.

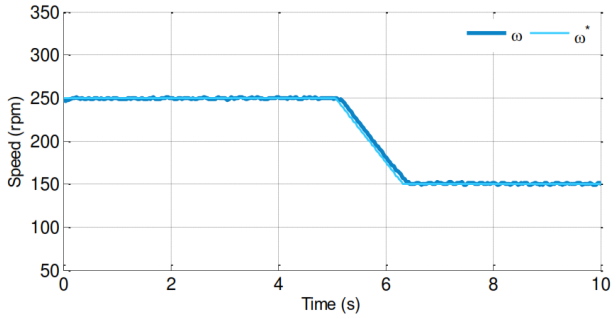

(a)

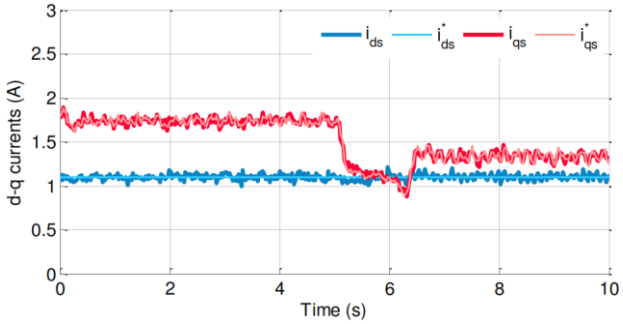

(b)

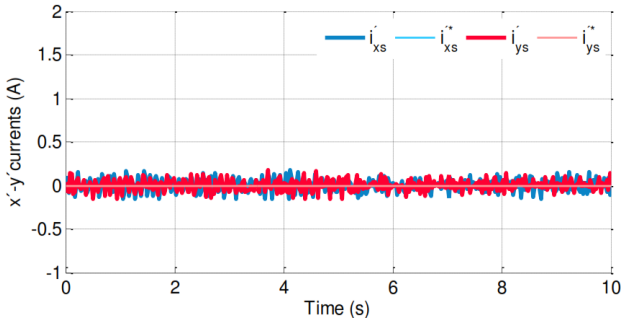

(c)

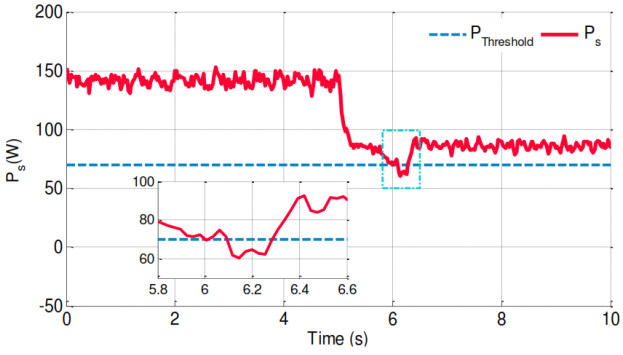

(d)

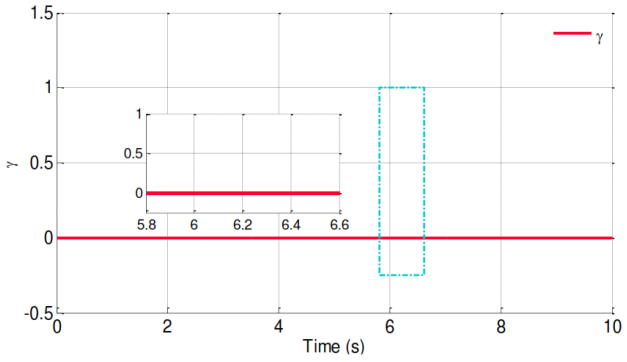

(e)

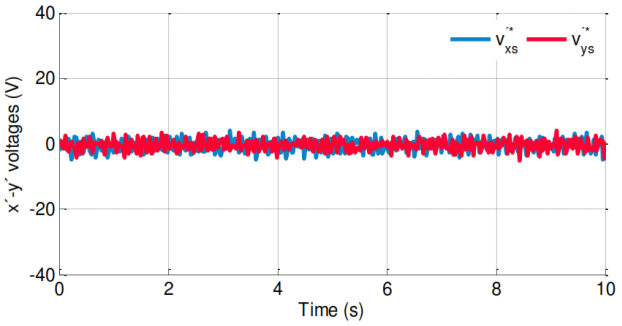

(f)

Fig. 5. Experimental results without *x-y* current injection during braking: (a) motor speed (ω_r), (b) *d-q* currents, (c) *x'-y'* currents, (d) stator power (P_s), (e) amount of injection (γ) and (f) *x'-y'* voltage references.

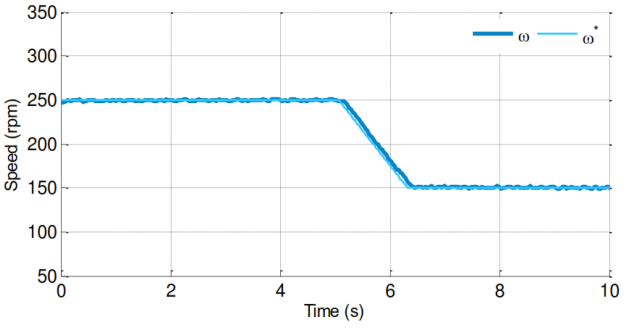

(a)

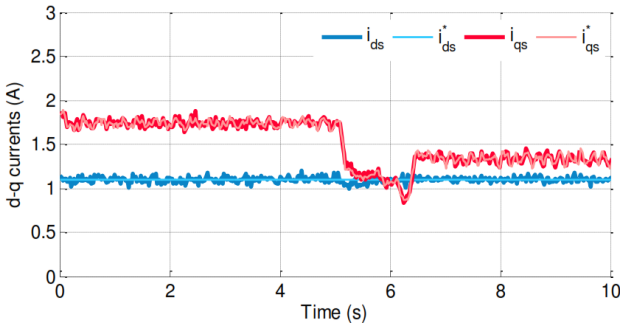

(b)

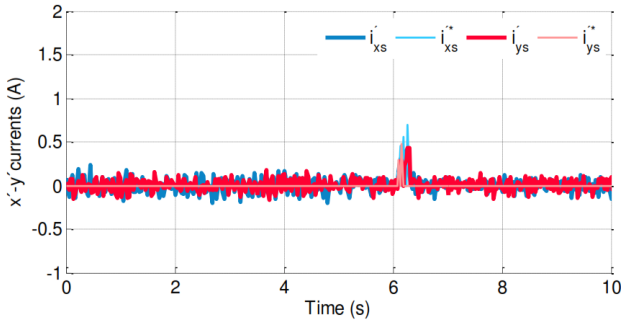

(c)

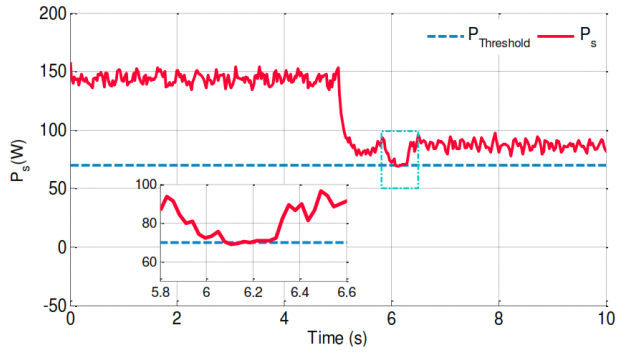

(d)

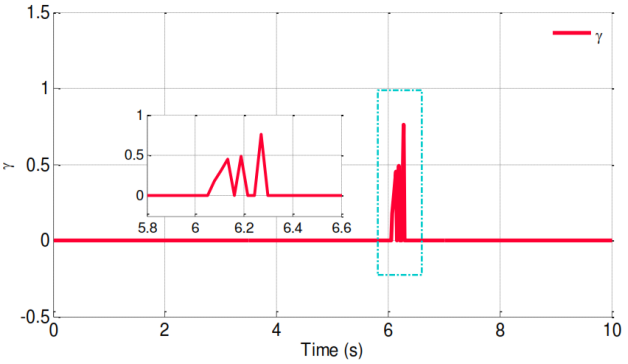

(e)

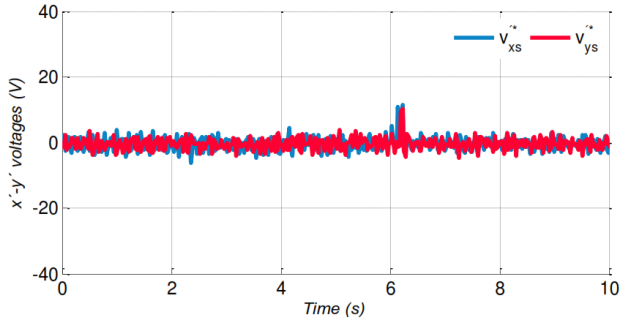

(f)

Fig. 6. Experimental results with *x-y* current injection during braking: (a) motor speed (ω_r), (b) *d-q* currents, (c) *x'-y'* currents, (d) stator power (P_s), (e) amount of injection (γ) and (f) *x'-y'* voltage references.

- The low impedance in the *x-y* plane allows the injection of circulating currents in a quick manner with low voltage requirements.

- Modifications in the control scheme are kept to a minimum. Since FOC strategies already include controllers that regulate *x-y* currents to zero in normal operation, it is only necessary to include a loss controller that activates the injection below a certain power threshold.

Even though the manner to inject the *x-y* currents may differ, the method is generally valid for any multiphase machine with distributed windings.

REFERENCES

1. M.J. Yang, H.L. Jhou, B-Y. Ma and K.K. Shyu (2009). "A cost-effective method of electric brake with energy regeneration for electric vehicles," IEEE Trans. on Industrial Electronics, vol. 56, no. 6, pp. 2203-2212.

2. E. Jung, H. Yoo, S. Sul, H. Choi and Y. Choi (2012). "A nine-phase permanent magnet motor drive system for an ultrahigh-speed elevator," IEEE Trans. on Industry Applications, vol. 48, no. 3, pp. 987-995.

3. R. Cárdenas, E. Espina, J. Clare and P. Wheeler (2015). "Self-tuning resonant control of a seven-leg back-to-back converter for interfacing variable speed generators to four-wire loads," IEEE Trans. on Industrial Electronics, vol. 62, no. 7, pp. 4168-4629.

4. A. Calle-Prado, S. Alepuz, J. Bordonau, P. Cortes and J. Rodriguez (2016). "Predictive control of a back-to-back NPC converter-based wind power system;" IEEE Trans. on Industrial Electronics, vol. 63, no. 7, pp. 4615-4627.

5. H.S. Che, E. Levi, M. Jones, M.J. Duran, W.P. Hew and N.A. Rahim (2014). "Operation of a six-phase induction machine using series-connected machine-side converters," IEEE Trans. on Industrial Electronics, vol. 61, no. 1, pp. 164-176.

6. ABB Drives Group (2011). Technical guide No. 8. Electrical braking. Chapter 1, pp. 7-9.

7. M. Hinkkanen and J. Luomi (2006). "Braking scheme for vector controlled induction motor drives equipped with diode rectifier without braking resistor," IEEE

Trans. on Ind. Appl., vol. 42, no. 5, pp. 1257-1263.

8. M. Swamy, T. Kume, Y. Yukihira, S. Fujii, M. Sawamura (2004). "A novel stopping method for induction motors operating from variable frequency drives," IEEE Trans. on Power Electronics, vol. 19, no. 4 pp. 11001107.

9. Y. Wang, T. Ito and R.D. Lorentz (2014). "Loss manipulation capabilities of deadbeat-direct torque and flux control induction machine drives," in Proc. of the Energy Conversion Congress and Exposition (ECCE), pp. 5100-5107.

10. I. Gonzalez-Prieto, M.J. Duran, F. Barrero, M. Bermudez and H. Guzman (2016). "Impact of post-fault flux adaptation on six-phase induction motor drives with parallel converters," IEEE Trans. on Power Electronics, early access, DOI: 10.1109/TPEL.2016.2533719, 2016.

11. A. Taheri, A. Rahmati and S. Kaboli (2012). "Efficiency improvement in DTC of six-phase induction machine by adaptive gradient descent of flux," IEEE Trans. on Power Electronics, vol. 27, no. 3, pp. 1552–1562.

12. J. Jiang and J. Holtz (2001). "An efficient braking method for vector controlled AC drives with a diode rectifier front end", IEEE Trans. on Industry Applications vol. 37, no. 5, pp. 1299-1307.

13. M. Rastogi and P. W. Hammond (2002). "Dual-frequency braking in AC drives," IEEE Trans. Power Electronics, vol. 17, no. 6, pp. 1032–1040.

14. E. Levi (2016). "Advances in converter control and innovative exploitation of additional degrees of freedom for multiphase machines," IEEE Trans. On Industrial Electronics, vol 63, no. 1, pp. 433-448.

15. F. Barrero and M.J. Duran (2016). "Recent advances in the design, modeling and control of multiphase machines – Part 1," IEEE Trans. on Industrial Electronics, Vol. 63, No. 1, pp. 449-458.

16. M.J. Duran and F. Barrero (2016). "Recent advances in the design, modeling and control of multiphase machines – Part 2," IEEE Trans. on Industrial Electronics, vol 63, no. 1, pp. 459-468.

17. Y. Zhao and T. A. Lipo (2012). "Space vector PWM control of dual three-phase induction machine using vector space decomposition," IEEE Trans. On Industry Applications, vol. 31, no. 5, pp. 1100–1109, Sep./Oct. 1995.

19. W. Cao, B.C. Mecrow, G.J. Atkinson, J.W. Bennett and D.J. Atkinson (2012). "Overview of electric motor technologies used for more electric aircraft (MEA)," IEEE Trans. on Industrial Electronics, vol. 59, no. 9, pp. 35233531.

19. B. C. Mecrow, A. G. Jack, D. J. Atkinson, S. R. Green, G. J. Atkinson. A. King and B. Green (2004). "Design and testing of a four-phase fault-tolerant permanent-magnet machine for an engine fuel pump," IEEE Trans. On Energy Conversion, Vol. 19, No. 4.

20. M. Mengoni, A. Tani, L. Zarri, G. Serra and D. Casadei (2012). "Position Control of a Multi-Motor Drive Based on Series-Connected Five-Phase Tubular PM Actuators," IEEE Trans. on Industry Applications, Vol. 48, No. 6.

21. A. Sivert, F. Betin, M. Moghadasian, A Yazidi and G. A. Capolino (2012). "Position Control of Six-Phase Induction Motor using Fuzzy Logic: Application to Electric Power Steering" XXth International Conference on Electrical Machines ICEM, Maseille, France.

22. I. Subotic, N. Bodo, E. Levi, M. Jones and V. Levi (2016). "Isolated chargers for EVs incorporating six-phase machines," IEEE Trans. on Industrial Electronics, vol. 63, no. 1, pp. 653-664.

23. H. Guzmán, M.J. Duran, F. Barrero, B. Bogado and S. Toral (2014). "Speed control of five-phase induction motors with integrated open-phase fault operation using model-based predictive current control techniques," IEEE Trans. on Industrial Electronics, vol. 61, no. 9, pp. 4474-4484.

24. H.S. Che, M.J. Duran, E. Levi, M. Jones, W.P. Hew and N.A. Rahim (2014). "Post-fault operation of an asymmetrical six-phase induction machine with single and two isolated neutral points," IEEE Trans. on Power Electronics, vol. 29, no. 10, pp. 5406-5416.

25. M.J. Duran, I. Gonzalez-Prieto, F. Barrero, M. Mengoni, L. Zarri and E. Levi (2015). "A simple braking method for six-phase induction motor drives with diode front-end rectifier," Industrial Electronics Society,

IECON 2015 – 41st Annual Conference of the IEEE, 9-12 Nov. 2015.

26. A. Yepes, J.A. Riveros, J. Doval-Gandoy, F. Barrero, O. Lopez, B. Bogado, M. Jones, E. Levi (2012). “Parameter identification of multiphase induction machines with distributed windings-part 1: sinusoidal excitation methods,” IEEE Trans. on Energy Conversion, vol. 27, no. 4, pp. 1056-1066.

27. J.A. Riveros, A. Yepes, F. Barrero, J. Doval-Gandoy, B. Bogado, O.Lopez, M. Jones, E. Levi (2012). “Parameter identification of multiphase induction machines with distributed windings-part 2: time-domain techniques,” IEEE Trans. on Energy Conversion, vol. 27, no. 4, pp. 1067-1077.

Mario J. Duran was born in Malaga, Spain, in 1975. He received the M.Sc. and Ph.D. degrees in Electrical Engineering from the University of Malaga Spain, in 1999 and 2003, respectively. He is currently an Associate Professor with the Department of Electrical Engineering at the University of Malaga. His research interests include modeling and control of multiphase drives and renewable energies conversion systems.

Ignacio Gonzalez Prieto was born in Malaga, Spain, in 1987. He received the Industrial Engineer and M. Sc. degrees from the University of Malaga, Spain, in 2012 and 2013, respectively. He obtained the PhD degree in Automatic and Electronic Engineering from the University of Seville, Spain, in 2016. He is currently a researcher in the Department of Electrical Engineering at the University of Malaga. His research interests include multiphase machines, fault detection methods, wind energy systems and electrical vehicles.

Federico Barrero (M 04; SM 05) received the MSc and PhD degrees in Electrical and Electronic Engineering from the University of Seville, Spain, in 1992 and 1998, respectively. In 1992, he joined the Electronic Engineering Department at the University of Seville, where he is currently an Associate Professor. He received the Best Paper Awards from the IEEE Trans. on Ind. Electron. for 2009 and from the IET Electric Power Applications for 2010-2011.

Emil Levi (S’89, M’92, SM’99, F’09) received his MSc and the PhD degrees in Electrical Engineering from the University of Belgrade, Yugoslavia in 1986 and 1990, respectively. From 1982 till 1992 he was with the Dept. of Elec. Engineering, University of Novi Sad. He joined Liverpool John Moores University, UK in May 1992 and is since September 2000 Professor of Electric Machines and Drives. He served as a Co-Editor-in-Chief of theIEEE Trans. on Industrial Electronics in the 2009-2013period and is currently Editor-in-Chief of the IET Electric Power Applications and an Editor of the IEEE Trans. on Energy Conversion. He is the recipient of the Cyril Veinott award of the IEEE Power and Energy Society for 2009 and the Best Paper award of the IEEE Trans. On Industrial Electronics for 2008. In 2014 he received the “Outstanding Achievement Award” from the European Power Electronics (EPE) Association.

Luca Zarri (M’05, SM’12) received the M. Sc. In Electrical Engineering, with honors, and the Ph.D.

degree from the University of Bologna, Bologna, Italy, in 1998 and 2007, respectively. He worked as a freelance software programmer from 1989 to 1992 and as a plant designer with a local engineering company from 1998 to 2002. In 2003 he became a Laboratory Engineer with the Department of Electrical Engineering, University of Bologna. Since 2014 he has been an Assistant Professor with the Department of Electric, Electronic and Information Engineering of the University of Bologna. He is author or co-author of more than 140 scientific papers. His research activity concerns the control of power converters and electric drives. He is a member of the IEEE Industry Applications, IEEE Power Electronics and IEEE Industrial Electronics Societies. At present, he is the Secretary of the Industrial Drives Committee of the IEEE Industry Application Society.

Michele Mengoni (M'13) was born in Forlì, Italy, in 1981. He received the M.S. and Ph.D. degrees in electrical engineering (with honors) from the University of Bologna, Bologna, Italy, in 2006 and 2010, respectively. He is currently an Assistant Professor with the Department of Electric, Electronic and Information Engineering "G. Marconi", University of Bologna. His research interests include design, analysis, and control of three phase electric machines, multiphase drives, and ac/ac matrix converters.

Corresponding Author

M. J. Duran*

Senior Member, IEEE, Department of Electrical Engineering, University of Malaga, Malaga, Spain

mjduran@uma.es